TECTONICS, VOL. 8, NO. 4, PAGES 865-880, AUGUST 1989

$^{40}Ar/^{39}Ar$ AGE CONSTRAINTS ON DEFORMATION AND METAMORPHISM IN THE MAIN CENTRAL THRUST ZONE AND TIBETAN SLAB, EASTERN NEPAL HIMALAYA

Mary S. Hubbard[1]

Department of Earth, Atmospheric and Planetary Sciences, Massachusetts Institute of Technology, Cambridge

T. Mark Harrison

Department of Geological Sciences, State University of New York at Albany

Abstract. In eastern Nepal, structural and petrologic observations suggest that movement on the Main Central Thrust (MCT), the development of an inverted metamorphic sequence, and leucogranite plutonism were genetically related. Samples from across the MCT zone and its hanging wall, the Tibetan Slab, were collected from four locations in the Everest region for $^{40}Ar/^{39}Ar$ studies: (1) the MCT zone, (2) the lower Tibetan Slab, (3) the upper Tibetan Slab away from intrusive rocks, and (4) the upper Tibetan Slab adjacent to and including leucogranitic material. Within the MCT zone, muscovite and hornblende yield cooling ages of 12.0±0.2 Ma and 20.9±0.2 Ma, respectively. K-feldspar gives a minimum age of 8.0±0.2 Ma (closure temperature (T_C) =220±15°C). In the lower Tibetan Slab a sample from a sheared pegmatite yields muscovite and biotite isochron ages of 7.7±0.4 Ma and 7.5±0.6 Ma and a K-feldspar minimum age of 6.4±0.8 Ma (T_C=225±20°C). An adjacent gneiss yields a 9.1±0.2 Ma biotite isochron and a K-feldspar minimum age of 3.6±0.2 Ma (T_C=210±50°C). In the upper Tibetan Slab, samples collected >200 m from visible intrusives yield a biotite isochron age of 20.2±0.2 Ma and a complex hornblende age spectrum suggestive of excess argon. At the fourth location an augen gneiss, a pegmatite, and a tourmaline-bearing leucogranite, all in mutual contact, yield indistinguishable mineral ages. The average biotite and muscovite isochron ages for these samples are 17.0±1.4 and 16.6±0.2 Ma, respectively. The minimum age for K-feldspar from the leucogranite is 15.5±1.8 Ma. As thermobarometric data from the MCT zone in this area suggest synmetamorphic deformation at temperatures of ~500°-550°C, the MCT hornblende (T_C=~500°C) dates this event at ~21 Ma. Diffusion experiments on hornblendes from the MCT zone provide data which support a maximum duration of peak metamorphic temperatures of ≤2 Ma. Biotite ages as old as ~20 Ma from the upper Tibetan Slab near leucogranites indicate that leucogranite intrusion was essentially coeval with deformation and metamorphism in the MCT zone. Very young ages in a ductile shear zone in the lower Tibetan Slab suggest that there has been deformation within the Tibetan Slab that postdates major movement on the MCT.

[1]Now at Geologisches Institute, ETH Zentrum, Zürich, Switzerland.

Paper number 89TC00708.
0278-7407/89/89TC-00708$10.00

INTRODUCTION

Collision between the Indian and Eurasian continents occurred between ~40 and 50 Ma [Molnar, 1984]. Convergence between these two continents has continued to the present, creating the spectacular Himalayan range and the elevated Tibetan Plateau. The original zone of collision, the Indus-Tsangpo suture, is marked by ophiolitic rocks in southern Tibet. The high peaks and rugged topography of the Himalaya coincide with metamorphic and intrusive rocks within the Indian plate. These crystalline rocks are part of the upper plate to a major, north- dipping thrust known as the Main Central Thrust (MCT).

The MCT is a major intracontinental fault zone that accomodated portions of the postcollisional convergence between India and Eurasia. This structure may have accomodated more than 100 km of displacement [Gansser, 1981]. It has been proposed that movement on the MCT may have influenced metamorphism and the development of leucogranites in the Himalaya [LeFort, 1975, 1981]. Unfortunately, these hypotheses have remained virtually untestable because relative and absolute ages of metamorphism, thrusting, and leucogranitic emplacement are lacking. Many of the leucogranites have been dated (see LeFort et al. [1987] for summary and Copeland et al. [1988b] for a discussion of possible ambiguities in age assessment), but the timing of metamorphism and deformation along the MCT has not been studied in detail.

In the Everest area of eastern Nepal the MCT is a thrust zone in which temperatures reached 500°-700°C during thrusting [Hubbard, 1989]. Amphibolite occurs in the lower part of the zone where calculated temperatures are close to the closure temperature for the K-Ar system in hornblende (~500°C). This coincidence provides an opportunity to date thrust movement and to compare this age with the ages of metamorphism within the hanging wall and with the ages of leucogranites. In this paper we report the results of a regional $^{40}Ar/^{39}Ar$ study of hornblende, biotite, muscovite, and potassium feldspar from the MCT zone and its upper plate.

GEOLOGIC SETTING

Three laterally continuous, north-dipping thrusts have been identified in the Himalaya: (1) the southernmost, and possibly seismically active, Main Frontal Thrust, (2) the Main Boundary Thrust, and (3) to the north the Main Central Thrust. The Main Frontal thrust separates terraced alluvial deposits from the overriding Early Miocene - Late Pleistocene age molassic rocks, locally known as the Siwaliks [Gansser, 1981]. To the north the Siwaliks are overridden along the Main Boundary Thrust (MBT) by the Lesser Himalayan sequence, which consists of a predominantly clastic sedimentary sequence of Precambrian to late Paleozoic age, although fossil control is scarce [Stöcklin, 1980]. This sequence generally has been metamorphosed to a low grade, but local areas remain unmetamorphosed . The Main Central Thrust (MCT) forms the northern boundary of the Lesser Himalaya (Figure 1). The upper plate to this structure is the Tibetan Slab with high-grade sillimanite-bearing gneissic rocks which have been subjected to widespread anatexis and intruded by leucogranitic material. Rocks adjacent to the MCT are characterized by an inverted metamorphism such that metamorphic grade increases toward structurally higher levels [Gansser, 1964; Pêcher, 1977; Hodges et al., 1988]. These rocks generally dip homoclinally to the north, thus the metamorphic grade increases northward. A variety of ideas have been proposed that link the inverted metamorphism with deformation along the MCT [LeFort, 1975; Maruo and Kizaki,1983; Brunel and Kienast, 1986]. In central Nepal, LeFort [1981] proposed that the formation and emplacement of the Manaslu leucogranite in the Tibetan Slab is also related to movement on the MCT. Radiometric ages, from a variety of techniques, range from 14.3±0.6 to 25.0±0.5 Ma (2-sigma uncertainties are reported herein for all radiometric ages) for intrusives within the Tibetan Slab [Schärer et al., 1986; Deniel et al., 1987], although Copeland et al. [1988a] have criticized the basis for assessment of many of the older ages. Movement on the MCT is generally thought to predate movement on the MBT, although no unambiguous age constraints exist for the temporal development of either structure.

Study Area

The structural setting and tectonic stratigraphy of the Everest region are described in detail by Hubbard [1988]. In

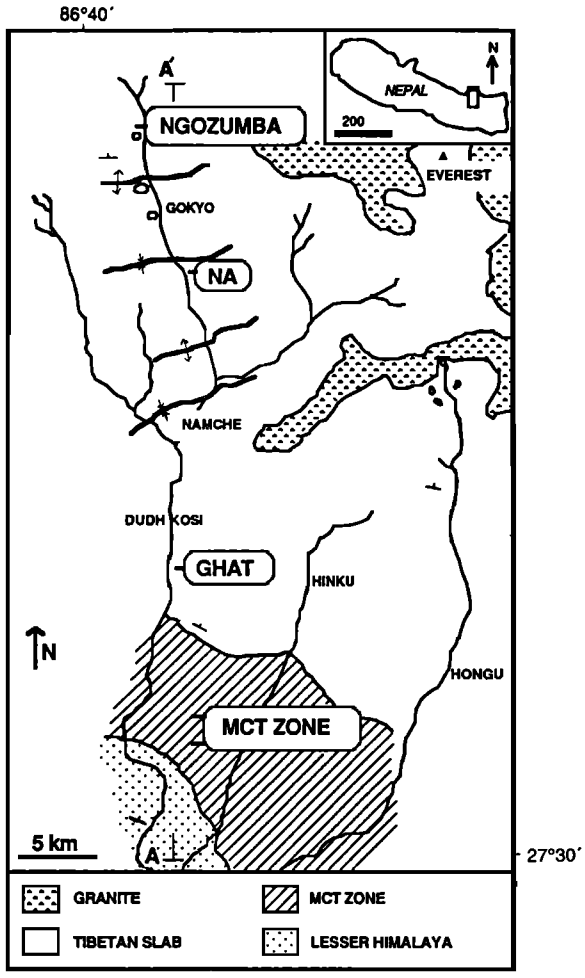

Fig. 1. Simplified geologic map of the study area in eastern Nepal. Sample locations for $^{40}Ar/^{39}Ar$ study are indicated by the circled place names. Samples 87H13F, 87H13E, 87H12C, and 87H12B are from the Main Central Thrust (MCT) zone. Samples 87H21C, and 87H21D are from Ghat. Samples 87H19A, and 87H19B are from Na. Samples 87H18A, 87H18B, and 87H18C are from Ngozumba.

general, the MCT in this area is a 3- to 5- km-thick, north- dipping shear zone consisting of a variety of lithologies including augen gneiss, slate, phyllite, quartzite, talc-schist, amphibolite, pelitic schist, calc-silicate rock, and banded biotite gneiss. Metamorphic grade increases up-structure, or northward, from chlorite-bearing schist in the Lesser Himalaya, which contains garnets in the upper ~100 m, through the staurolite and kyanite isograds in the lower MCT zone, to sillimanite-bearing gneiss in the upper MCT zone and across the Tibetan Slab. Metamorphic isograds and lithologic contacts are roughly parallel to the dominant schistosity.

The lower boundary of the MCT zone is a lithologic contact between an augen gneiss in the MCT zone and a chlorite-muscovite schist in the uppermost Lesser Himalaya. The Lesser Himalayan section is a thick sequence of fine-grained psammite, schist, and quartzite. Locally, biotite and garnet occur in the uppermost unit of chlorite-muscovite schist.

The upper boundary of the MCT zone is within a biotite gneiss unit at a level that separates highly sheared rocks of the thrust zone from overlying, less-deformed but migmatized gneissic rocks of the Tibetan Slab. Shear zones do exist north of the MCT zone, but deformation does not appear to be as widespread. Lithologies within the Tibetan Slab include biotite gneiss, calc-silicate rock, quartzite, augen gneiss, granitic gneiss and pelitic schist. Garnet and sillimanite are common in pelitic and gneissic rocks throughout this section. Anatectic granites and small-scale granitic intrusions occur in the lower Tibetan Slab, but the frequency and volume of granitic material increases toward the north. There are several large leucogranitic bodies in this region, such as the south face of Nuptse or the Makalu massif, but the majority of the granitic material occurs in networks of dikes and sills. Some of the larger intrusive bodies have retained xenoliths of the country rock. Schistosity within these xenoliths has often remained parallel to the country rock schistosity in the area. Crosscutting relationships in the dikes and sills suggest multiple generations of intrusion.

Metamorphism

Metamorphic assemblages across the MCT zone and into the Tibetan Slab suggest an increase in metamorphic grade toward higher structural levels. Mineral rim thermobarometric data [Hubbard, 1989] from samples across the MCT zone and lower Tibetan Slab in eastern Nepal show an increase up-structure in temperatures of metamorphic equilibration from 505°±50°C (2-sigma uncertainty) in the lower MCT zone to 725°±96°C at about 1.5 kilometers structurally above the upper boundary of the MCT zone (Figure 2). Above that level temperatures decrease to 593°±50°C at ~8 km structurally above the MCT zone.

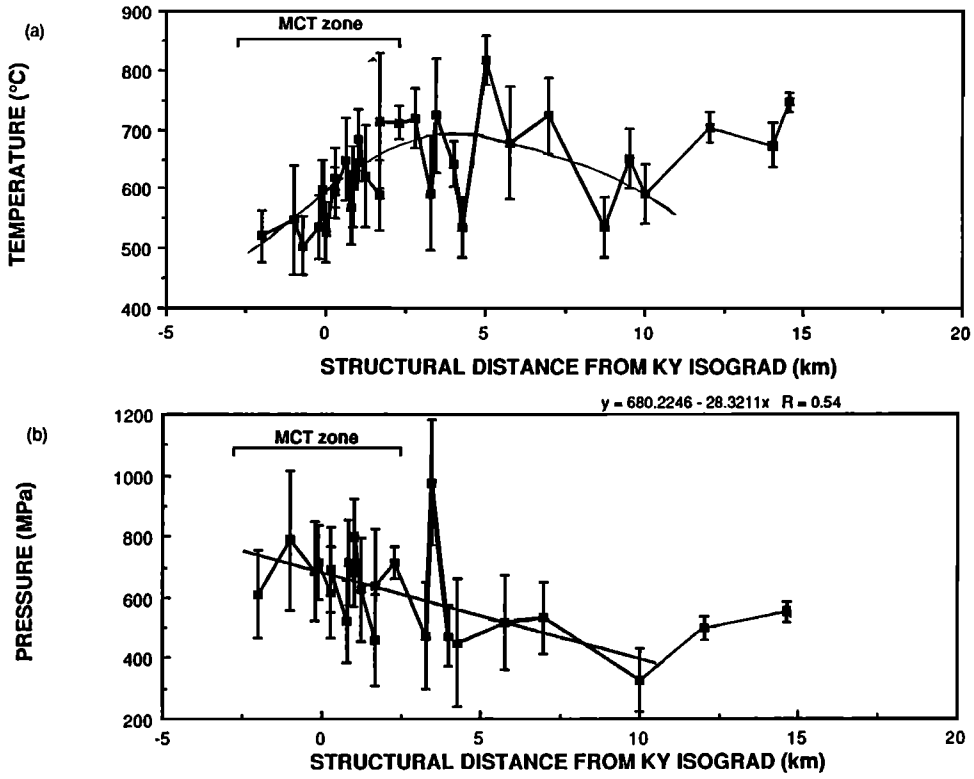

Fig. 2. Summary of thermobarometric data plotted against structural distance from the kyanite isograd [from Hubbard, 1989] (a) temperature, (b) pressure.

Pressures across the same section decrease from 685±160 MPa in the lower MCT zone to 328±102 MPa at ~8 km above the MCT zone (Figure 1). These data support the model of LeFort [1975] that metamorphism was synchronous with movement on the MCT.

In the upper Tibetan Slab, metamorphic temperatures and pressures from samples across a folded section are nearly uniform, with average values of 712°C and 533 MPa. It has been proposed [Hubbard, 1989] that these samples either came from one structural horizon, thus experiencing identical uplift histories, or they may have been heated during the period of leucogranitic intrusion in this area. In the latter case, regional metamorphism in the upper Tibetan Slab would be the result of advection of heat during intrusion.

PREVIOUS GEOCHRONOLOGY

Tertiary Granites of the Everest Area

A small number of workers have attempted to obtain ages of the Tertiary leucogranites in eastern Nepal using a variety of techniques. Because of limitations of the individual techniques there has been a mixed degree of success. Table 1 summarizes the majority of existing age data for this region.

Ferrara et al. [1983] used the Rb-Sr method to obtain both whole- rock isochrons and mineral isochron ages for samples from the south side of the peaks Nuptse and Lhotse. Two suites of samples gave whole- rock ages of 52±1 Ma and 13.7±7 Ma. One of the samples from the 52 Ma suite yielded a 17.3±0.3 Ma internal isochron from K-feldspar, biotite, muscovite, and whole rock. Another sample, not included in either whole- rock isochron, had an internal four-mineral isochron age of 16.5±0.5 Ma. Ferrara et al. suggested that the middle Miocene ages could represent a period of regional uplift, but they also recognize that Sr heterogeneity may be a problem in Himalayan leucogranites.

Schärer et al. [1986] determined a monazite U-Pb age of 14.4±0.6 Ma from an undeformed granite sample from the north side of Mount Everest. This age is

TABLE 1. Previous Geochronologic Results, Mount Everest Region

System	Location	Rock Type	Mineral	Age*	Source
Rb/Sr	Lhotse glacier	leucogranite	whole rock	52±1 Ma	1
Rb/Sr	Lhotse glacier	leucogranite	whole rock/biotite muscovite/K-feldspar	17.3±0.3 Ma	1
Rb/Sr	Nuptse glacier	leucogranite	whole rock	14±7 Ma	1
Rb/Sr	Lhotse glacier	leucogranite	whole rock/biotite tourmaline/K-feldspar muscovite	16.5±0.5 Ma	1
Rb/Sr	near Na	orthogneiss	whole rock/biotite	15.6±0.6 Ma	1
Rb/Sr	near Na	orthogneiss	whole rock/biotite	15.3±0.6 Ma	1
Rb/Sr	Lhotse glacier	paragneiss	whole rock/biotite	16.4±0.3 Ma	1
U/Pb	Mount Everest	leucogranite	monazite	14.4±0.6 Ma	2
U/Pb	Makalu	leucogranite	monazite	21.9±0.2 Ma	3
U/Pb	Makalu	leucogranite	monazite	24.0±0.4 Ma	3
U/Pb	north side Everest	leucogranite	zircon/monazite	20±1 Ma	4
$^{40}Ar/^{39}Ar$	north side Everest	leucogranite	biotite	17.1±0.2 Ma	4
$^{40}Ar/^{39}Ar$	north side Everest	leucogranite	muscovite	16.7±0.4 Ma	4
$^{40}Ar/^{39}Ar$	north side Everest	leucogranite	K-feldspar	16.2±0.2 Ma	4
K-Ar	Lho La Pass	leucogranite	biotite	19±2 Ma	5
K-Ar	Pumori	leucogranite	biotite	47±5 Ma	5
K-Ar	Everest basecamp	leucogranite	biotite	19±2 Ma	5
K-Ar	north side Nuptse	mica schist	biotite	17.0±1.6 Ma	5
K-Ar	north side Nuptse	amphibolite	hornblende	24±2 Ma	5
K-Ar	north side Nuptse	biotite gneiss	biotite	18.0±1.6 Ma	5
K-Ar	north side Nuptse	amphibolite	amphibole	56±4 Ma	5
K-Ar	Pangboche	amphibolite	biotite	40±4 Ma	5
K-Ar	Pangboche	amphibolite	hornblende	350±40 Ma	5
K-Ar	Tyangpoche	biotite gneiss	biotite	16.0±1.8 Ma	5
K-Ar	south of Namche	augen gneiss	biotite	13.4±1.2 Ma	5
K-Ar	south of Namche	migmatite	biotite	10.5±2.0 Ma	5
K-Ar	south of Namche	migmatitic diorite	biotite	10±2 Ma	5
K-Ar	south of Ghat	biotite gneiss	biotite	14.0±1.0 Ma	5
K-Ar	Puiyan (MCT) zone	augen gneiss	biotite	9.0±1.0 Ma	5
K-Ar	Puiyan (MCT) zone	biotite gneiss	biotite	5.5±0.6 Ma	5
K-Ar	north of KhariLa(MCT)	biotite gneiss	biotite	3.4±0.2 Ma	5
K-Ar	south of KhariLa(MCT)	mica schist	biotite	8.5±0.8 Ma	5

* With two sigma uncertainty.

Sources: 1, Ferrara et al. [1983]; 2, Schärer et al. [1986]; 3, Schärer [1984]; 4, Copeland et al. [1987]; 5, Krummenacher et al. [1978]

considerably younger than zircon and monazite crystallization ages determined by Copeland et al. [1988b] from neighboring Everest granites at 20±1 Ma and ages of 21.9±0.2 Ma and 24.0±0.4 Ma determined by Schärer [1984] on monazites from granites of the Makalu massif, roughly 20 km to the southeast. These age differences may result from multiple intrusive events.

Copeland et al. [1987] used the $^{40}Ar/^{39}Ar$ technique on biotite, muscovite, and K-feldspar from a granite just north of Everest and obtained cooling ages of 17.1±0.2, 16.7±0.4, and 16.2±0.2 Ma, respectively. Similar K-Ar ages were determined by Krummenacher et al. [1978] on two biotite separates from granites near the Everest base camp in Nepal at 19±2. Krummenacher et al. [1978] also measured a 47±5 Ma biotite from a granite in the Everest region. This latter age could either represent an older intrusion or reflect excess Ar.

Metamorphic Rocks of the Tibetan Slab

Ferrara et al. [1983] attempted to determine the age of gneissic samples from the south face of Lhotse using Rb-Sr on whole- rock samples. Significant scatter in the data did not permit calculation of a meaningful age but rather was interpreted as indicating isotopic heterogeneity in the sedimentary protolith. They did obtain an age of 16.4±0.3 Ma from a biotite-whole- rock pair that is consistent with the ages of leucogranites from the same area.

Krummenacher et al. [1978] obtained K-Ar biotite ages on schistose and gneissic rocks from across the Tibetan Slab. In general, their ages range from 10.5±2.0 to 18.0±1.6 Ma. With a few exceptions the ages tend to decrease structurally downsection. One anomalously old age of 40±4 Ma may be due to excess Ar.

Copeland et al. [1988b] found "inherited" monazite in a leucogranite

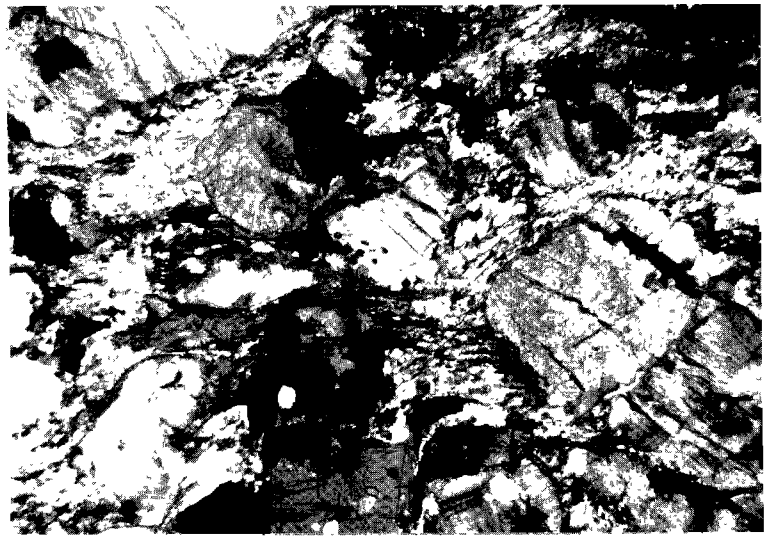

Fig. 3. Protomylonitic texture in pegmatite from Ghat. Field of view is 13 mm.

sample from northwest of Everest that revealed an upper intercept of 471±10 Ma, suggesting a protolith in the Tibetan Slab of at least that age. Inherited zircon from the same rock yielded source ages as young as ~500 Ma.

Metamorphic Rocks of the MCT Zone

Krummenacher et al. [1978] determined four K-Ar ages on biotite from samples within the region that has been defined in this paper as the MCT zone. These ages range from 3.4±0.2 to 9.0±1.0 Ma, suggesting more recent cooling at this level than within the upper Tibetan Slab.

SAMPLING

In order to reveal the cooling- age pattern across this region, samples were collected from four areas (Figure 1): (1) the MCT zone, (2) the lower Tibetan Slab (a locality referred to as Ghat), (3) the upper Tibetan Slab away from intrusive rocks (a locality referred to as Na), and (4) the upper Tibetan Slab adjacent to and including leucogranitic intrusions (a locality referred to as Ngozumba). Multiple rock types from each location were chosen in an effort to maximize the number of datable minerals, thus maximizing the cooling history data for that area.

MCT zone

Four samples were collected in the MCT zone. Sample 87H13F is an augen gneiss from the lowest unit in the MCT zone. In this sample, K-feldspar porphyroclasts (<1cm) are set in a foliated matrix of biotite, muscovite and recrystallized quartz. Sample 87H13E was collected ~5 m from 87H13F in a psammite horizon within this lower augen gneiss. The psammite contains the assemblage garnet-staurolite-biotite-quartz. Garnets are anhedral and poikiloblastic. Samples 87H12B and 87H12C came from a small amphibolite layer within a mica schist in the midsection of the MCT zone. The assemblage of this amphibolite includes hornblende, biotite, quartz, calcite, sphene, and plagioclase. In sample 87H12C the biotite grains are oriented and concentrated in thin layers that define the foliation.

Lower Tibetan Slab: Ghat

Two adjacent samples were chosen in the lower Tibetan Slab just south of the village of Ghat. Sample 87H21C is a biotite gneiss with an assemblage of quartz, plagioclase, biotite, and K-feldspar. This sample has domains of fine-grained recrystallized quartz and occasional myrmekitic textures which may be associated with deformation [LaTour, 1987]. Sample 87H21D is a pegmatite which appeared undeformed in the field, but when observed in thin section it shows a protomylonitic texture (Figure 3). Relict K-feldspar grains are surrounded by a fine-grained matrix of recrystallized quartz, biotite, and muscovite. Tourmaline is also present in 87H21D.

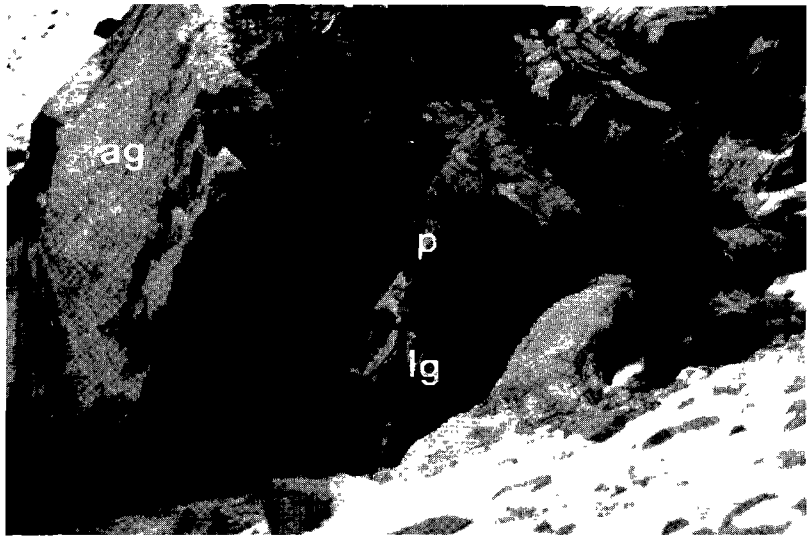

Fig. 4. Outcrop that was sampled at Ngozumba. The augen gneiss (ag), pegmatite (p), and leucogranite (lg) are labeled.

Upper Tibetan Slab: Na

Two samples were collected south of Na in the Gokyo valley at a site > 200 m from visible leucogranitic intrusives. The intent was to analyze samples from this structural level whose thermal history reflects uplift and not intrusion. Sample 87H19A is an amphibolite and 87H19B is a tourmaline-bearing biotite gneiss. Both samples are foliated but neither shows evidence of intense deformation.

Upper Tibetan Slab: Ngozumba

The outcrop at Ngozumba (Figure 4), in the upper Gokyo valley, consists of an augen gneiss (87H18A) that is intruded by pegmatite sills (87H18B) and cut by a tourmaline-bearing leucogranite (87H18C). Myrmekites are present in the augen gneiss and the pegmatite. The pegmatite and the leucogranite contain chlorite, and muscovite is sericitized in the augen gneiss, the pegmatite, and the leucogranite.

ANALYTICAL TECHNIQUES

Mineral separates were obtained using standard magnetic and heavy liquid separation techniques. Sample preparation, irradiation, and analytical procedures are the same as those described by Harrison and Fitz Gerald [1986]. Correction factors to account for interfering nuclear reaction products are given, together with the analytical results for each sample, in Appendix 1, available on microfiche[1].

Closure temperatures for hornblende, biotite, and muscovite were estimated from hydrothermal diffusion studies (see McDougall and Harrison [1988] for a review). Closure temperatures for K-feldspars were calculated using the diffusion parameters estimated from measured ^{39}Ar release during laboratory heating. Three of the K-feldspars yielded reasonable values for closure temperature. Unfortunately, the K-feldspars from gneissic and granitic rocks of the upper Tibetan Slab were partly sericitized and gave unrealistically low closure temperatures. For these samples a closure temperature of 200°C was assumed, as this temperature is within the uncertainty of closure temperatures calculated for other K-feldspars of similar composition from the study area.

---

[1]Supplemental data are available with entire article on microfiche. Order from American Geophysical Union, 2000 Florida Avenue, N.W., Washington, DC 20009. Document T89-003; $2.50. Payment must accompany order.

RESULTS

MCT zone

Muscovite, biotite, and K-feldspar were analyzed from sample 87H13F, and biotite was analyzed from the adjacent sample 87H13E. Release spectra from both samples are shown in Figure 5. Biotite and muscovite from 87H13F yield plateaux at ~40 Ma and ~12 Ma, respectively. As biotite typically has a lower closure temperature than muscovite, this reversal suggests the presence of excess argon. Excess argon is a relatively common problem in biotites and, in certain cases, is not detectable with the isochron approach because of the high Ar solubility in biotite and high $^{40}Ar/^{36}Ar$ ratio of the trapped gas. Muscovite, however, generally appears less susceptible to the effects of excess argon, so we interpret the muscovite isochron age of 12.0±0.2 Ma to be a meaningful cooling age. The K-feldspar release spectrum is "saddle-shaped," which is also a sign of excess argon [Dalrymple et al., 1975; Harrison and McDougall, 1980]. The minimum age on this spectrum at ~8 Ma appears sensible given the consistency with the muscovite age. The closure temperature for this K-feldspar is calculated to be T_C=220±15°C.

Biotite was the only mineral analyzed in sample 87H13E. The release spectrum

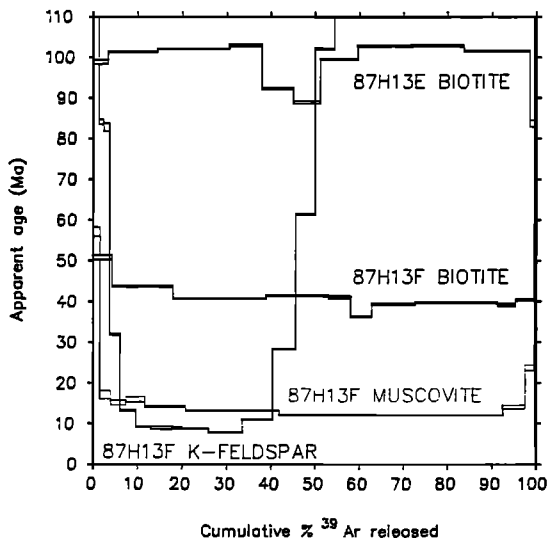

Fig. 5. Release spectra for mineral separates from samples 87H13E and 87H13F from the lower MCT zone.

(Figure 5) reveals clear age discordance and does not define a plateau. A 90-100 Ma total gas age predates continental collision and is therefore unlikely. This age is also inconsistent with the younger ages from sample 87H13F, which was collected just 5 m away. Excess argon must, again, be the cause of this unrealistically old age. The relatively flat but discordant age spectrum underscores the cautions recommended by Gaber et al. [1988] regarding age spectra interpretation from biotite.

The biotite from sample 87H12C yields a plateau age of ~60 Ma, which is considerably older than the hornblende age (Figure 6). The hornblende data are complicated by the presence of two, distinct, trapped argon components [Heizler and Harrison, 1988], but the sample yields an isochron age of 20.9±0.3 Ma (Figure 6). This age is consistent with the muscovite and K-feldspar ages from sample 87H13F collected at a slightly lower structural level within the MCT zone. The biotite does not yield any simple correlations.

A hornblende separate from sample 87H12B gives a complex release spectrum (Figure 7) which could be interpreted as an excess Ar uptake profile superimposed on an Ar loss profile from a Paleozoic age [e.g., Harrison and McDougall, 1980] or as "saddle- shaped" due to excess Ar [e.g., Harrison and McDougall, 1981], in which case no chronological meaning could be inferred from the spectrum. We suggest that the former explanation is correct and have performed laboratory heating experiments to test this conclusion.

Preirradiated, coarse-grained, aliquants of 87H12B and 87H12C hornblendes were hydrothermally treated for 416 hours at 800°C and 1 kbar. Following the heat treatment, the ^{39}Ar concentrations of both samples were determined relative to their starting materials, allowing calculation of D/a^2, which is the ratio of Ar diffusivity (D) to the square of the diffusion radius (a). We chose to use ^{39}Ar rather than $^{40}Ar^*$ (*radiogenic) for this purpose, as the nonuniform $^{40}Ar^*$ distribution implicit in Figure 7 would seriously compromise assumptions required to calculate model diffusion coefficients [Crank, 1975]. The measured losses for 87H12B and 87H12C of 6 and 18%, respectively, correspond to values of D/a^2 of $2x10^{-10}$ and $2x10^{-9}$ cm^2/s, respectively.

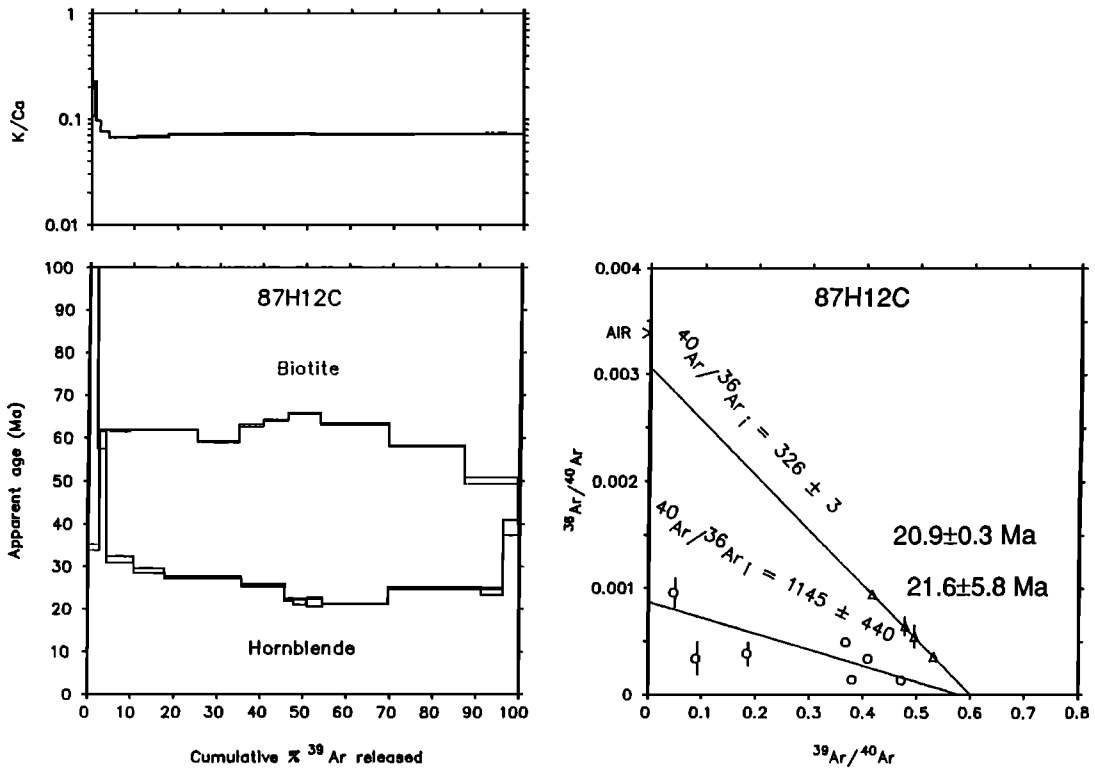

Fig. 6. Release spectra for biotite and hornblende from sample 87H12C (MCT zone), shown together with the K/Ca plot and isochron plot for the hornblende. Two trapped components yield isochrons that indicate roughly the same age.

Similar values for ^{37}Ar loss (7 and 15%, respectively) strongly suggest that the Ar loss is from the hornblende rather than some other phase. We note that the measured $^{40}Ar^*$ loss for 87H12C was similar to the ^{39}Ar loss due to the uniform distribution of both (Figure 6), but that $^{40}Ar^*$ loss in 87H12B was appreciably higher, possibly due to the preferential degassing of excess ^{40}Ar held in near boundary sites.

The contrast in D/a^2 of an order of magnitude is likely a consequence of differing diffusion radii between the two samples. Baldwin and Harrison [1988] have shown that metamorphic hornblende with variable Fe/Mg contents, when subjected to hydrothermal treatment similar to that utilized for 87H12B and 87H12C, yield an activation energy for Ar transport of ~60 kcal/mol but contain broadly varying diffusion dimensions (controlled by exsolution, defect structure, cleavage, fractures, etc.) that strongly effect overall Ar loss. Since our samples 87H12B and 87H12C were collected from the same outcrop, they must have experienced similar thermal histories but responded to Ar loss quite differently. From Figure 7 we can infer that the rising age gradient in the latter portion of gas release for 87H12B reflects 50% Ar loss from an original age of ~450 Ma (suggested to us by the data of Copeland et al. [1988b]), whereas sample 87H12C was virtually completely degassed (say >95%). Figure 8 shows the relationship between fractional Ar loss and $\pi Dt/a^2$ (where t is time) for a variety of geometries. Viewing the hornblende crystals as spherical in shape (see Harrison [1981] and Baldwin and Harrison [1988] for an explanation), we can see from Figure 8 that a combined $\pi^2 Dt/a^2$ parameter of 0.3 would effect the observed 50% Ar loss in 87H12B hornblende. Since we know that for an equivalent temperature and heating duration 87H12C hornblende would have a $\pi^2 Dt/a^2$ value ten times higher (i.e., 3), from Figure 8 we infer an Ar loss in excess of 95%, similar

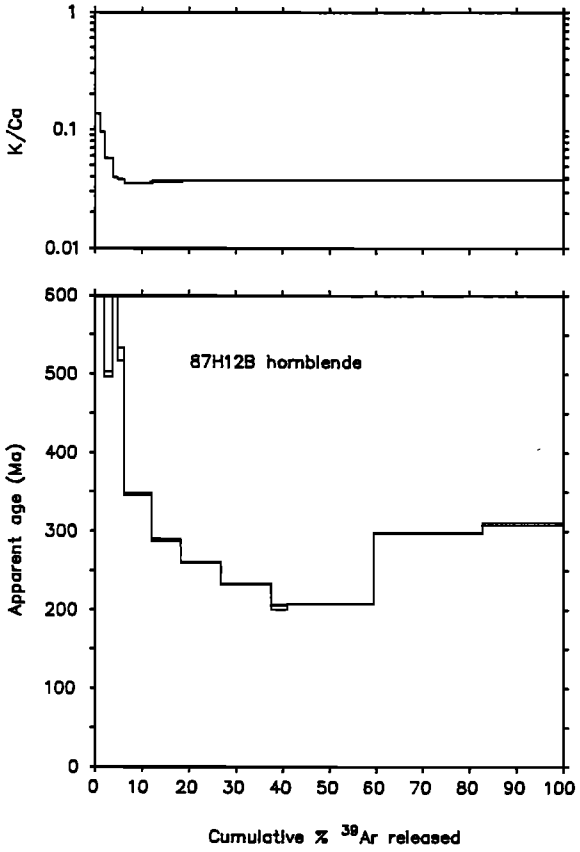

Fig. 7. Release spectra and K/Ca plot for hornblende from sample 87H12B (MCT zone).

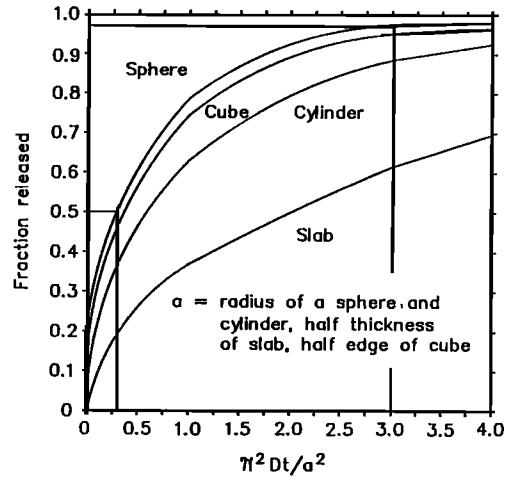

Fig. 8. Plot of fraction Ar loss versus π^2Dt/a^2 for a variety of geometries.

to that observed. Thus our hypothesis that the latter portion of the 87H12B hornblende age spectrum represents incomplete degassing rather than excess Ar incorporation appears justified on the basis that (1) the form of the spectrum differs from our common expectation of excess Ar (see McDougall and Harrison [1988] for review), (2) the degree of ^{40}Ar loss during laboratory heating suggests excess ^{40}Ar in a near boundary siting, (3) the flat K/Ca plot (Figure 7) is not indicative of the exsolved structures needed to yield "saddle-shaped" spectra, but if, however, there are fine-grained intergrowths containing excess Ar, then recoil homogenization may tend to damp this effect, and (4) the relative ^{39}Ar losses from adjacent samples (87H12B and 87H12C) suggest a higher Ar retentivity for 87H12B.

Lower Tibetan Slab: Ghat

K-feldspar from sample 87H21C gives a minimum age from the release spectrum (Figure 9) of 3.6±0.2 Ma (T_C = 210±50), whereas biotite yields an isochron age of 9.1±0.2 Ma. Sample 87H21D is from the adjacent sheared pegmatite and yields a K-feldspar minimum age of 6.4±0.8 Ma (Figure 10). Biotite and muscovite isochrons from 87H21D give ages of 7.5±0.6 Ma and 7.7±0.4 Ma, respectively. The behavior of the spectra for the K-feldspars from these two

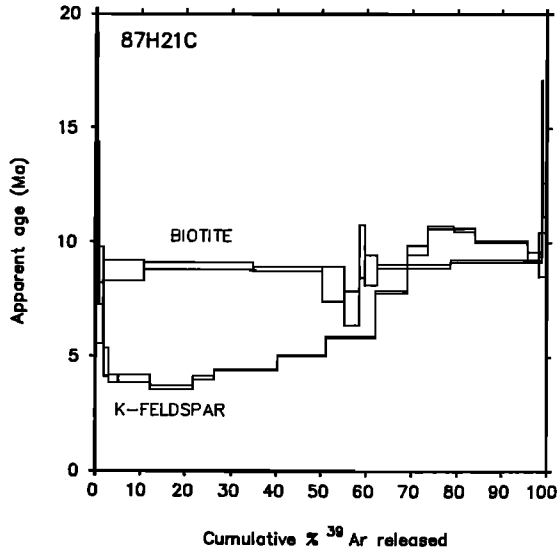

Fig. 9. Release spectra for biotite and K-feldspar from sample 87H21C (Ghat).

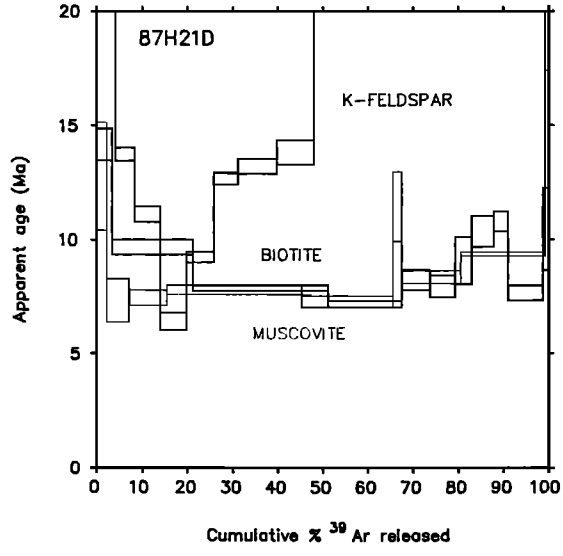

Fig. 10. Release spectra for muscovite, biotite, and K-feldspar from sample 87H21D (Ghat).

samples are markedly different. Almost 50% of the ^{39}Ar released is younger than 5 Ma for sample 87H21C, with the remaining gas fraction younger than 15 Ma. For sample 87H21D, less than 50% of the ^{39}Ar released from the K-feldspar is younger than 15 Ma, with the remaining gas fractions older than 20 Ma. Sample 87H21D appears to have been affected by excess argon.

Upper Tibetan Slab: Na

Release spectra for hornblende from sample 87H19A and biotite from sample 87H19B are shown together in Figure 11a. The age spectum for the hornblende suggests marginal excess argon uptake with a minimum age on the spectrum of 22.7±4.4 Ma. A biotite isochron age for the second through ninth increments gives an age of 20.2±0.2 Ma (mean square of weighted deviates (MSWD)=16, trapped $^{40}Ar/^{36}Ar$=299±10). A second analysis of the hornblende (Figure 11b) reveals a similar age spectrum to the first run but in detail is more diagnostic of excess argon in the high-temperature steps.

Upper Tibetan Slab: Ngozumba

Biotite and K-feldspar were analyzed from sample 87H18A, an augen gneiss in the upper Tibetan Slab (Figure 12). The

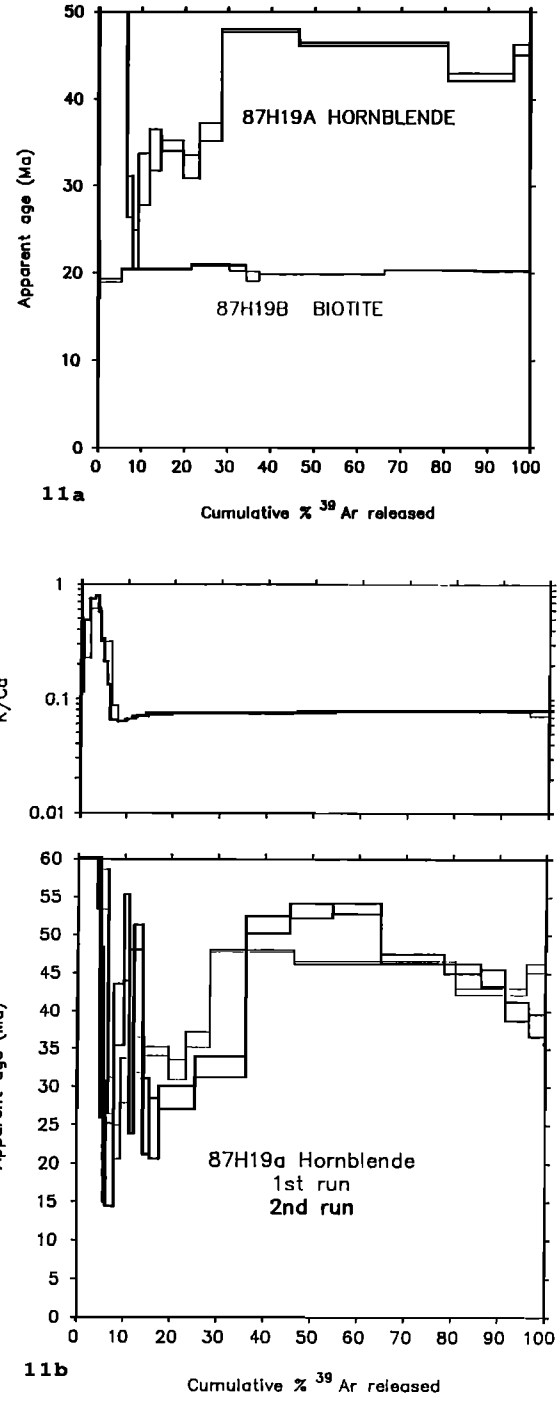

Fig. 11. (a) Release spectra for biotite from sample 87H19B and hornblende first run from sample 87H19A (Na), (b) Release spectra for hornblende second run, 87H19A.

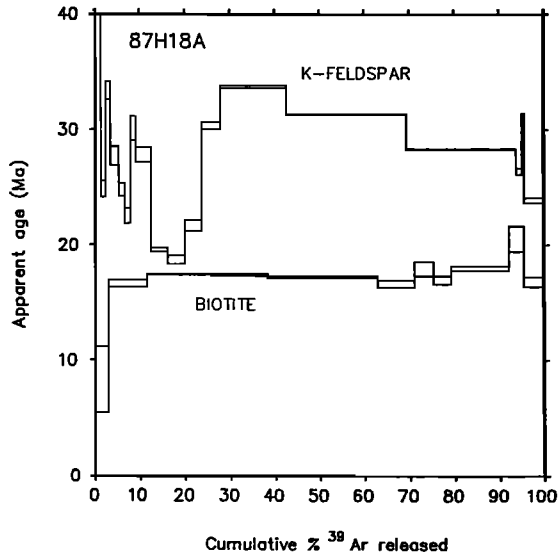

Fig. 12. Release spectra for biotite and K-feldspar from sample 87H18A (Ngozumba).

release spectrum for K-feldspar is irregular and, again, suggestive of excess argon. The minimum age on this spectrum is 18.7±0.8 Ma, which is older than the biotite isochron age of 17.2±0.8 Ma (steps 2-10, MSWD=5, trapped $^{40}Ar/^{36}Ar$=301±11).

Cooling ages were obtained for muscovite, biotite, and feldspar from the pegmatite sample 87H18B from Ngozumba (Figure 13). As in sample 87H18A, the feldspar age spectrum is irregular and yields a minimum age (21.7±0.8 Ma) which is older than the mica ages from this sample. The biotite and muscovite isochron ages are nearly indistinguishable at 16.8±1.4 Ma (steps 1-11, MSWD=33.7, trapped $^{40}Ar/^{36}Ar$=308±3) and 17.0±0.4 Ma (steps 2-10, MSWD=4.2, trapped $^{40}Ar/^{36}Ar$=285±18), respectively. The biotite release spectrum is somewhat irregular, and there is scatter about the isochron as indicated by the high MSWD. K-feldspar and muscovite release spectra for the leucogranitic sample 87H18C are shown in Figure 14. Again the K-feldspar spectrum is irregular, but in this sample the minimum age of 15.5±1.8 Ma is younger than the muscovite isochron age of 16.6±0.4 (steps 1-11, MSWD=2.1, $^{40}Ar/^{36}Ar$=304±4).

TECTONIC IMPLICATIONS

A summary of the mineral ages from this study are given in Table 2. As discussed in the previous section, some of these ages may reflect excess argon and are therefore less likely to be actual cooling ages. From the subset of data considered meaningful a representative age for each mineral, from each site, was plotted versus mineral closure temperature (Figure 15). Taken together, these ages should reveal a consistent pattern from which tectonic rates and timing can be inferred.

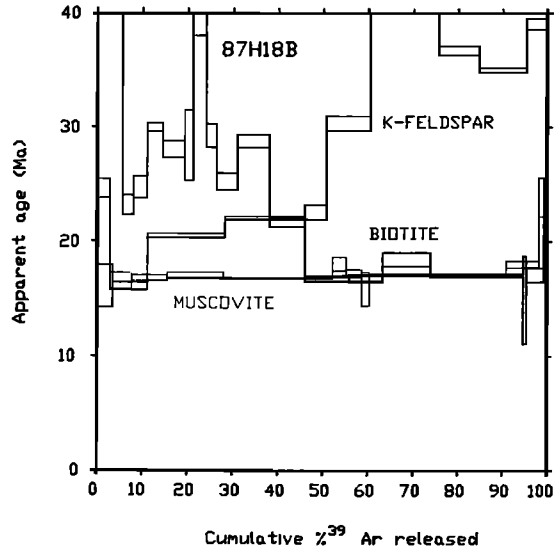

Fig. 13. Release spectra for muscovite, biotite, and K-feldspar for sample 87H18B (Ngozumba).

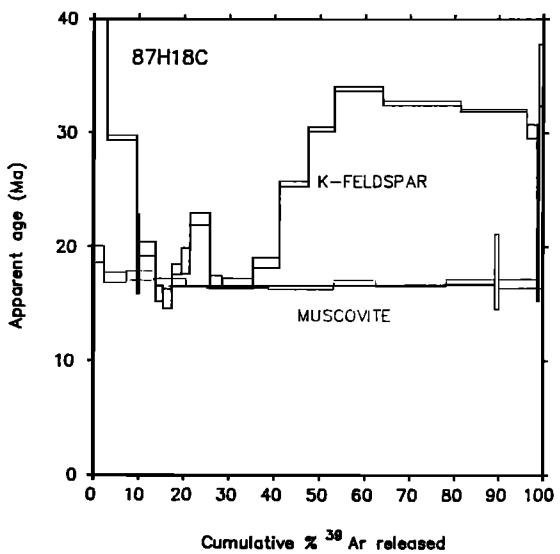

Fig. 14. Release spectra for muscovite and K-feldspar for sample 87H18C (Ngozumba).

TABLE 2. Summary of $^{40}Ar/^{39}Ar$ Ages

Sample	Rock Type	Mineral	Age	Closure Temperature
		MCT zone		
87H13F*	augen gneiss	K-feldspar	8.0±0.2 Ma (M)	220±15°C
87H13F	augen gneiss	biotite	36.3±0.4 Ma (M)	300±50°C
87H13F*	augen gneiss	muscovite	12.0±0.2 Ma (I)	350±50°C
87H13E	biotite gneiss	biotite	88.8±0.6 Ma (M)	300±50°C
87H12C	amphibolite	biotite	58.3±3.4 Ma (I)	300±50°C
87H12C*	amphibolite	hornblende	20.9±0.2 Ma (I)	500±50°C
87H12B	amphibolite	hornblende	204.0±5.2 Ma (M)	500±50°C
		Ghat		
87H21C*	biotite gneiss	K-feldspar	3.6±0.2 Ma (M)	210±50°C
87H21C	biotite gneiss	biotite	9.1±0.2 Ma (I)	300±50°C
87H21D	pegmatite	K-feldspar	6.4±0.8 Ma (M)	225±20°C
87H21D*	pegmatite	biotite	7.5±0.6 Ma (I)	300±50°C
87H21D*	pegmatite	muscovite	7.7±0.4 Ma (I)	350±50°C
		Na		
87H19B*	biotite gneiss	biotite	20.2±0.2 Ma (I)	300±50°C
87H19A*	amphibolite	hornblende	22.7±4.4 Ma (M)	510±50°C
		Ngozumba		
87H18A	augen gneiss	K-feldspar	18.7±0.8 Ma (M)	250(?)
87H18A	augen gneiss	biotite	17.2±0.8 Ma (I)	300±50°C
87H18B	pegmatite	K-feldspar	21.7±0.8 Ma (M)	250(?)
87H18B*	pegmatite	biotite	16.8±1.4 Ma (I)	300±50°C
87H18B	pegmatite	muscovite	17.0±0.4 Ma (I)	350±50°C
87H18C*	leucogranite	K-feldspar	15.5±1.8 Ma (M)	250(?)
87H18C*	leucogranite	muscovite	16.6±0.4 Ma (I)	350±50°C

(I) is age determined from isochron and (M) is age from minimum on release spectra.

* Data plotted in Figure 15.

If our interpretation of the age spectrum for 87H12B hornblende is correct (see results section), we can use our knowledge of the diffusion properties and metamorphic temperatures to constrain the duration of heating. Our Ar loss experiments imply a frequency-factor/diffusion-dimension parameter (D_o/a^2) of ~1500, assuming an activation energy of 65 kcal/mol [Harrison, 1981]. Metamorphic temperatures for this portion of the MCT (Figure 1a) are in the range ~500°-550°C. An estimate of the maximum duration of heating can be made from Figure 8 which shows that ~50% Ar loss requires a $\pi^2 Dt/a^2$ value of ~0.3. Our diffusion parameters lead us to calculate a $(D/a^2)_{500°C}$ of 5×10^{-15} cm^2/s, which translates to a time at peak temperature of ~0.25 Ma, although a parabolic temperature history could yield a duration of ~2.50 Ma. Shorter durations result for higher temperatures. In the lower MCT zone, peak metamorphic temperatures are interpreted as synchrous with movement on the thrust [Hubbard, 1989]. The isochron age of our less retentive hornblende (87H12C) of 20.9±0.2 Ma, with a closure temperature that falls within the range of metamorphic temperatures, likely reflects the age of thrust movement at the culmination of this metamorphism.

In the upper Tibetan Slab, similar ages (15-20 Ma) to that of the MCT were recorded at Na and Ngozumba in the upper Tibetan Slab by biotite, muscovite, and K-feldspar separates. These ages are consistent with 17-19 Ma K-Ar biotite ages [Krummenacher et al., 1978] and 16-17 Ma Rb/Sr whole rock mineral isochrons [Ferrara et al., 1983] for granite samples from the Everest area in Nepal but are somewhat younger than the U-Pb monazite and zircon ages of 20±1 Ma obtained by Copeland et al. [1988b] for a granite sample from just north of Mount Everest. Although field evidence suggests that the leucogranites in the Everest region represent multiple generations, the collective geochronologic data suggest that MCT metamorphism and deformation was generally coeval with leucogranitic

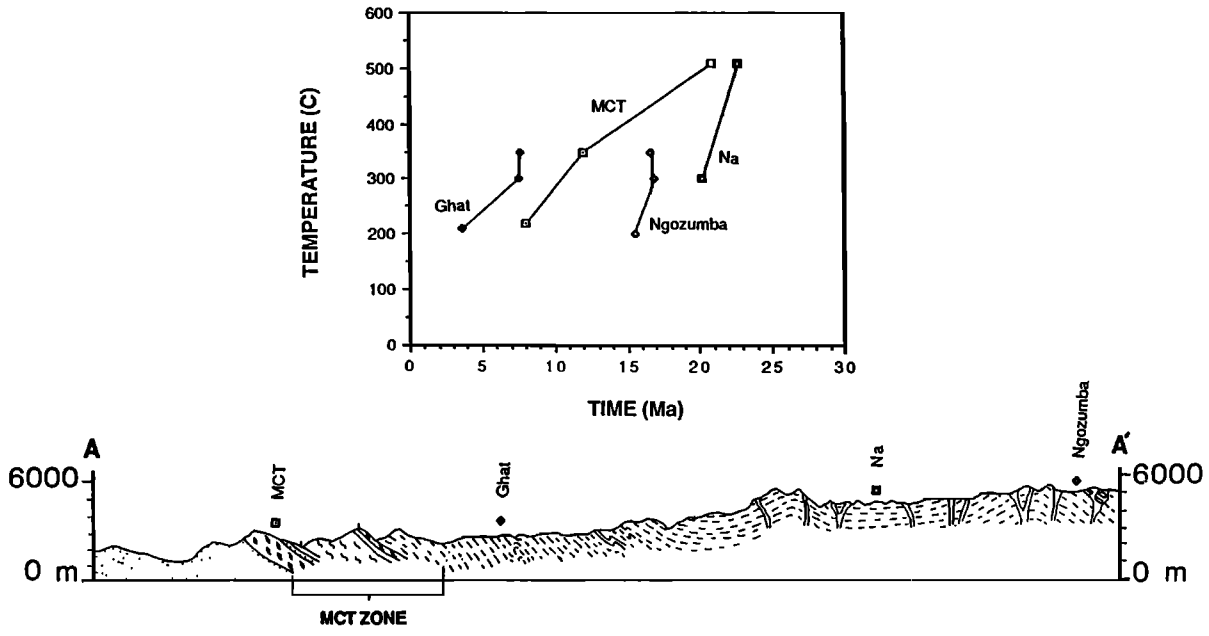

Fig. 15. Plot of age versus closure temperature for mineral separates from the MCT zone, Ghat, Na, and Ngozumba. Cross section provides structural reference for sample locations. Sample number and source of age (isochron or minimum from release spectra) are given in Table 2.

intrusion in the upper Tibetan Slab.

The samples from Na were collected some distance (>200 m) from any observable intrusive rocks and permit us to examine the thermal history of the upper Tibetan Slab away from the direct influence of the leucogranites. Unfortunately, the hornblende age spectrum (Figure 11a) is complex and duplication (Figure 11b) strongly suggests contamination by excess Ar. No age significance should be placed on the ~40-55 Ma ages. The 20.2±0.2 Ma biotite from Na (Figure 11a) is slightly older than the ~17 Ma mica ages from Ngozumba, but the significance of this age difference is difficult to assess in view of the problematic nature of our other biotite age spectra from this study.

Biotite and muscovite from a mylonitized pegmatite at Ghat record ~8 Ma ages, which constrains the age of deformation to be not younger than ~8 Ma. Cooling by uplift of the inverted metamorphic sequence would produce mineral ages which would become younger monotonically from north to south. The four mica ages from Ngozumba yield an age of 16.9±0.3 Ma, similar to mica ages from the leucogranite belt farther west [Copeland et al., 1988a]. However, the mica ages at Ghat of ~8 Ma are from an intermediate position between the MCT zone to the south, with a muscovite age (deemed the most reliable) of 12.0±0.2 Ma, and the Na/Ngozumba region in the north, with ~17 Ma ages. This age progression reversal suggests either (1) emplacement of this slab from depth along unrecognized structures since 8 Ma or (2) localized deformation between ~12 and ~8 Ma accompanied by hot fluid circulation sufficient to reset the mica ages. Whichever the case, this deformation indicates that there has been localized shear deformation within the Tibetan Slab and that this deformation significantly postdates movement of the MCT.

CONCLUSIONS

In the Everest region of eastern Nepal a $^{40}Ar/^{39}Ar$ hornblende age from the MCT zone suggests thrust movement and metamorphism at ~21 Ma. Mica ages from a leucogranite and adjacent gneiss within the Tibetan Slab suggest that granitic intrusion was contemporaneous with MCT thrusting and metamorphism. These data are consistent with the LeFort [1981] model of granite generation associated

with movement on the MCT. Peak temperatures were probably maintained for less than ~2 Ma.

A biotite from the upper Tibetan Slab away from intrusives is ~20 Ma, only slightly older than biotite ages from the leucogranites and adjacent gneisses and reflects regional heating associated with leucogranitic intrusion.

The ~8 Ma mica ages from a shear zone in the lower Tibetan Slab indicate relatively recent deformation in the Higher Himalaya, which may have also been important in shaping the tectonic history of this area.

Acknowledgments. We wish to thank Kip Hodges, Peter Molnar, Leigh Royden, Clark Burchfiel, and Gary Johnson for useful discussions and comments on an early version of this manuscript. R.J. Fleck, T.C. Onstott, B.M. Page, and an anonymous reviewer are gratefully acknowledged for helpful reviews. Thanks go to Sange Dorje Sherpa and Mountain Travel Nepal for logistical support during sample collection and Matt Heizler for technical assistance. Matt, Lynn, and Ashley Heizler are thanked for their endless hospitality during data collection. This research was supported by the American Alpine Club, The Explorer's Club, The Geological Society of America, and NSF grants EAR-8414417 and EAR-8707569.

REFERENCES

Baldwin, S.L., and T. M. Harrison, Diffusion of ^{40}Ar in metamorphic hornblende, Eos Trans. AGU, 69, 522, 1988.

Brunel, M., and J.R. Kienast, Étude pétro-structurale des chevauchements ductile himalayens sur la transversale de L'Everest-Makalu (Népal oriental), Can. J. Earth Sci., 23, 1117-1137, 1986.

Copeland, P., T.M. Harrison, R. Parrish, B.C. Burchfiel, and K.V. Hodges, Constraints on the age of normal faulting, north face of Mt. Everest: Implications for Oligo-Miocene uplift (abstract), Eos Trans. AGU 68(44), 1444, 1987.

Copeland, P., T.M Harrison, and P. LeFort, Cooling history of the Manaslu granite, north-central Nepal (abstract), Geol. Soc. Am. Abstr. Programs, 20, 1988a.

Copeland, P., R. Parrish, and T.M.Harrison, Identification of inherited radiogenic Pb in monazite and its implications for U-Pb systematics, Nature, 333, 760-763, 1988b.

Crank, J., The Mathematics of Diffusion, 414 pp., Oxford University Press, New York, 1975.

Dalrymple, G.B., C.S. Gromme, and R.W. White, Potassium-Argon age and paleomagnetism of diabase dikes in Liberia: Initiation of central Atlantic rifting, Geol. Soc. Am. Bull., 86, 399-411, 1975.

Deniel, C., P. Vidal, A. Fernandez, P. Le Fort, and J. Peucat, Isotopic study of the Manaslu granite (Himalaya, Nepal): Inferences on the age and source of Himalayan leucogranites, Contrib. Mineral. Petrol., 96, 78-92, 1987.

Ferrara, G., B. Lombardo, and S. Tonarini, Rb/Sr geochronology of granites and gneisses from the Mount Everest region, Nepal Himalaya, Geol. Rundsch., 72(1), 119-136, 1983.

Gaber, L.J., K.A. Foland, and C.E. Corbato, On the significance of argon release from biotite and amphibole during $^{40}Ar/^{39}Ar$ vacuum heating, Geochim. Cosmochim. Acta, 32, 2457-2465, 1988.

Gansser, A., Geology of the Himalayas, 289 pp., Wiley-Interscience, New York, 1964.

Gansser, A., The geodynamic history of the Himalaya, in Zagros, Hindu Kush, Himalaya Geodynamic Evolution, edited by H.K. Gupta and F.M. Delany, Geodyn. Ser., vol. 3, pp. 111-121, AGU, Washington D.C., 1981.

Harrison, T.M., Diffusion of ^{40}Ar in hornblende, Contrib. Mineral. Petrol., 78, 324-331, 1981.

Harrison, T.M., and J.D. Fitz Gerald, Exsolution in hornblende and its consequences for $^{40}Ar/^{39}Ar$ age spectra and closure temperature, Geochim. Cosmochim. Acta, 50, 247-253, 1986.

Harrison, T.M., and I. McDougall, Investigations of an intrusive contact, northwest Nelson, N.Z., II, Diffusion of radiogenic and excess ^{40}Ar in hornblende revealed by $^{40}Ar/^{39}Ar$ age spectrum analysis, Geochim. Cosmochim. Acta, 44, 2005-2020, 1980.

Harrison, T.M., and I. McDougall, Excess argon in metamorphic rocks from the Broken Hill region, New South Wales: Implications for $^{40}Ar/^{39}Ar$ age spectra and the thermal history of the region,

Earth Planet. Sci. Lett., 55, 123-149, 1981.

Heizler, M., and T.M. Harrison, Multiple trapped argon isotope components revealed by $^{40}Ar/^{39}Ar$ isochron analysis, Geochim. Cosmochim. Acta, 52, 1295-1303, 1988.

Hodges, K.V., M.S. Hubbard, and D.S. Silverberg, Metamorphic constraints on the thermal evolution of the central Himalayan orogen, Philos. Trans. R. Soc. London, Ser A.326, 257-280, 1988.

Hubbard, M., Thermobarometry, $^{40}Ar/^{39}Ar$ geochronology, and structure of the Main Central Thrust zone and Tibetan Slab, Eastern Nepal Himalaya, Ph.D. thesis, 169 pp., Mass. Inst. of Technol., Mass., 1988.

Hubbard, M., Thermobarometric constraints on the thermal history of the Main Central Thrust Zone and Tibetan Slab, Eastern Nepal, J. Metamorph. Geol., 7, 19-30, 1989.

Krummenacher, D., A.M. Bassett, F.A. Kingery, and H.F. Layne, Metamorphism and K-Ar age determinations in eastern Nepal, in Tectonic Geology of the Himalaya, edited by P.S. Saklani, pp. 151-166, Today and Tomorrow's Printing. and publication, New Delhi, India, 1978.

La Tour, T.E., Geochemical model for the symplectic formation of myrmekite during amphibolite-grade progressive mylonitization of granite, Geol. Soc. Am Abstr. Programs, 19(7), 741, 1987.

Le Fort, P., Himalayas: The collided range, Present knowledge of the continental arc, Am. J.Sci. 275-A, 1-44, 1975.

Le Fort, P., Manaslu leucogranite: A collision signature of the Himalaya, A model for its genesis and emplacement, J. Geophys. Res., 86, B11, 10,545-10,568, 1981.

Le Fort, P., M. Cuney, C. Deniel, C. France-Lanord, S.M.F. Sheppard, B.N. Upreti, and P. Vidal, Crystal generation of the Himalayan leucogranites, Tectonophysics, 134, 39-57, 1987.

Maruo, Y., and K. Kizaki, Thermal structure in the nappes of the eastern Nepal Himalayas, in Granites of Himalaya, Karakorum and Hindu-Kush, edited by F.A. Shams, pp. 271-286, Punjab University, Lahore, Pakistan, 1983.

McDougall, I., and T.M. Harrison, Geochronology and thermochronology by the $^{40}Ar/^{39}Ar$ Method, 212 pp., Oxford University Press, New York, 1988.

Molnar, P., Structure and tectonics of the Himalaya: Constraints and implications of geophysical data, Annu. Rev. Earth Planet. Sci., 12, 489-518, 1984.

Schärer, U., The effect of initial ^{230}Th disequilibrium an young U-Pb ages: The Makalu case, Himalaya, Earth Planet. Sci. Lett., 67, 191-204, 1984.

Schärer, U., R.H. Xu, and C.J. Allègre, U-(Th)-Pb systematics and ages of Himalayan leucogranites, South Tibet, Earth Planet. Sci. Lett., 77, 35-48, 1986.

T. M. Harrison, Department of Geological Sciences, State University of New York at Albany, Albany, NY 12222.

M. S. Hubbard, Geologisches Institut, ETH Zentrum, CH-8092, Zürich, Switzerland.

(Received October 28, 1988;
revised March 9, 1989;
accepted April 5, 1989.)